



## Research article

## CDC73 serves as a tumour-promoting factor in oesophageal cancer

Jie Song<sup>a,1</sup>, Wenyong Guo<sup>b,1</sup>, Hua Xu<sup>c</sup>, Tao Gao<sup>c,\*</sup><sup>a</sup> Department of Cardiac surgery, Ningbo medical center Lihuli Hospital of Ningbo University, No.57, Xingning Road, Ningbo city 315041, Zhejiang Province, China<sup>b</sup> Department of Digestive, Ningbo medical center Lihuli Hospital of Ningbo University, No.57, Xingning Road, Ningbo city 315041, Zhejiang Province, China<sup>c</sup> Department of Thoracic Surgery, First Affiliated Hospital of Nanchang University, Nanchang city 330006, Jiangxi Province, China

## ARTICLE INFO

## Keywords:

Oesophageal cancer  
CDC73  
RRP15  
Cell proliferation  
Cell apoptosis

## ABSTRACT

The role of human cell division cycle 73 (CDC73) in human cancers has sparked controversy; however, its significance in oesophageal cancer remains elusive. This study aimed to elucidate CDC73 expression and its biological implications in human oesophageal cancer. Our findings unveiled a notable upregulation of CDC73 in both oesophageal cancer cell lines and tissues. Importantly, elevated CDC73 levels in patients with oesophageal cancer correlated with an unfavourable prognosis. Functional investigations revealed that CDC73 knockdown effectively curtailed the proliferation and growth of oesophageal cancer cells both *in vitro* and *in vivo*. Mechanistically, RRP15 emerged as a potential downstream target of CDC73 through a screening process involving identification of the top co-expressed genes, subsequent knockdown experiments, and observation of significant inhibition of cell proliferation, with RRP15 showing the most pronounced effect. This finding was further supported by the positive correlation observed between CDC73 and RRP15 in ESCA samples analysed using the ENCORI Pan-Cancer Analysis Platform. Notably, depletion of RRP15 in CDC73-overexpressing cells led to a shift from augmented to diminished tumour growth. Collectively, our findings underscore the pivotal role of CDC73 in oesophageal cancer through the modulation of RRP15 expression, suggesting CDC73 as a potential therapeutic target for treating oesophageal cancer.

## 1. Introduction

Oesophageal cancer, ranking eighth among the most common cancers globally, presents a significant challenge owing to its poor prognosis, placing sixth in terms of survival rate [1]. Its incidence has been on the rise, exacerbating the global health burden. The current clinical strategies include surgical resection, radiotherapy, and chemotherapy. However, despite these advancements, the mortality rate remains high because of the limited efficacy and severe adverse effects of conventional therapies [2]. Targeted therapies have emerged as promising alternatives [3]. For instance, cetuximab and bevacizumab have demonstrated improved outcomes by targeting the epidermal growth factor receptor and vascular endothelial growth factor respectively [4]. Nevertheless, these therapies face challenges, such as drug resistance and incomplete restoration of patient health. Hence, it is imperative to identify more effective targets for oesophageal cancer therapy and deepen our understanding of the underlying mechanisms.

\* Corresponding author.

E-mail address: [prof\\_gaotao@sina.com](mailto:prof_gaotao@sina.com) (T. Gao).<sup>1</sup> These authors contributed to this work equally.

Human cell division cycle 73 (CDC73), also known as parafibromin, is a nuclear protein comprising 531 amino acids encoded by the CDC73 gene located on chromosome 1q31.2 [5,6]. CDC73 mutations are linked to hyperparathyroid-jaw tumour (HPT-JT) syndrome, an autosomal dominant condition characterised by parathyroid tumours, fibro-osteomobular tumours, cystic nephropathy, and uterine tumours [7–9]. Additionally, CDC73 mutations have been implicated in breast, renal, gastric, and parathyroid cancers [10–13]. Despite the debate over its role in these cancers, no evidence has linked CDC73 function to the development of oesophageal cancer.

In this study, we explored the clinicopathological roles and functional significance of CDC73 expression in oesophageal cancer. By examining the proposed function of CDC73, we aimed to provide new evidence supporting its potential as a promising therapeutic target for treating oesophageal cancer.

## 2. Materials and methods

### 2.1. Ethics statement

This study involving human participants was approved by the Ethics Committee of Shanghai Outdo Biotech Company (No. SHYJS-CP-1407005), and all the patients provided signed informed consent. The animal experiments adhered to the regulations and guidelines approved by the Laboratory Animal Ethics Committee of Ningbo University (No. NBU20220097).

### 2.2. Cell lines and animals

In this study, both normal human oesophageal epithelial cells (HEEC) and four human oesophageal cancer cell lines (EC9706, KYSE450, Eca-109, and TE-1) were obtained from the American Type Culture Collection. HEEC and TE-1 cells were cultured in RPMI-1640 medium supplemented with 10 % FBS; EC9706 and Eca-109 cells were grown in DMEM supplemented with 10 % FBS, and KYSE450 cells were cultured in EMEM (MEM + NEAA) supplemented with 10 % FBS.

BALB/c nude mice (4 weeks old, female, weighing approximately 21 g) were procured from Beijing Weitong Lihua Experimental Animal Technical Co., Ltd. (Beijing, China). These mice were housed under controlled conditions with five mice per cage, maintaining a temperature of 22–25 °C, humidity of 50–60 %, and a 12-h light/dark cycle. Adequate water and food were provided ad libitum to ensure continuous access.

### 2.3. Immunohistochemistry (IHC)

The oesophageal cancer tissue microarray, comprising 80 cases of para-carcinoma tissue and 78 cases of tumour tissue, was supplied by Shanghai Outdo Biotech Co., Ltd. (Shanghai, China). Following deparaffinization, the samples were subjected to EDTA-based antigen retrieval (1 × EDTA; Beyotime Biotechnology Co., Ltd., Shanghai, China). To inhibit endogenous peroxidase activity, the sections were treated with 3 % H<sub>2</sub>O<sub>2</sub> for 5 min. Subsequently, the sections were incubated overnight at 4 °C with primary antibodies and then with appropriate secondary antibodies. Staining was performed using DAB for 5 min, followed by counterstaining with haematoxylin (Baso Diagnostics Inc., Zhuhai, China) for 10–15 s. Staining extent was graded on a scale of 0 (0 %), 1 (1–25 %), 2 (26–50 %), 3 (51–75 %), or 4 (76–100 %), with staining intensity ranging from weak to strong. Specimens were categorised as negative (0), positive (1–4), ++ positive (5–8), or +++ positive (9–12). The IHC score, which was determined independently by three pathologists, was used for quantitative analysis. High and low expression parameters were determined relative to the median immunohistochemical staining scores for the tumour tissues. Samples with scores less than or equal to the median were categorised as exhibiting low CDC73 expression, while those with scores greater the median were classified as demonstrating high CDC73 expression. Details of the antibodies used are provided in Supplementary table 1.

### 2.4. Lentivirus RNAi construction and packaging, and transfection of target cells by lentivirus

Short hairpin RNA interference sequences were designed based on the sequences of target genes. All vectors were provided by Shanghai Yibeirui Biomedical Science and Technology Co., Ltd. (Shanghai, China). Primers were designed to amplify the CDC73 gene sequence, which was then ligated into the LV-007 vector to construct a lentiviral vector overexpressing the CDC73 gene. For RRP15, NSL1, MARCH7, RPAP3 and UCHL5, oligo DNA sequence synthesis was performed by Shenggong Bioengineering Co. Ltd. (Shanghai, China). The CDC73 interference sequence was synthesised as a single-stranded DNA oligo. The synthesised single-stranded DNA oligos were dissolved in 100 mM annealing buffer (10 mM Tris, 50 mM NaCl, 1 mM EDTA) and subjected to a 90 °C water bath for 15 min, followed by natural cooling to room temperature to form sticky-ended double-stranded DNA. According to the NEB manual (Vector [1 µg/µL] 2 µL, CutSmart Buffer 5 µL, AgeI [10 U/µL] 1 µL, EcoR I [10 U/µL] 1 µL, H<sub>2</sub>O up to 50 µL), the linearisation of the BR-V108 vector was achieved by incubating it with AgeI and EcoR I restriction enzymes at 37 °C for 1 h. Subsequently, the linearised vector was ligated with the double-stranded DNA oligo using T4 DNA Ligase (Linearised Vector [100 ng/µL] 1 µL, Insert [100 ng/µL] 1 µL, 10 × T4 DNA ligase Buffer 2 µL, T4 DNA ligase 1 µL, H<sub>2</sub>O up to 20 µL) at 16 °C for 2 h. The resulting plasmid was introduced into TOP10 *E. coli* competent cells by adding 1 µg of plasmid per 10 µL of competent cells, followed by incubation in antibiotic-free LB medium at 37 °C and 200 rpm for 1 h. The transformed cells were then spread onto LB agar plates containing ampicillin and incubated overnight at 37 °C. Single colonies were picked and used as templates for PCR (Taq Plus DNA Polymerase 0.2 µL, 10 × Buffer 2 µL, Primer-F 0.4 µL, Primer-R 0.4 µL, Template -, H<sub>2</sub>O up to 20 µL) to confirm the presence of the desired DNA fragments. The PCR products were analysed on a 1 % agarose gel. Positive clones were sequenced, and clones with sequencing results entirely matching the target

sequence were selected. The correctly sequenced samples were transferred to 150 mL LB liquid medium containing Amp antibiotics and cultured overnight at 37 °C. The Plasmid was extracted according to the instructions of the EndoFree Maxi Plasmid Kit (TIANGEN, Cat. # DP118-2), and the qualified plasmid was subjected to downstream lentiviral infection and packaging. Sequences of the designed vectors, plasmids, and oligos were detailed in the Supplementary tables 2–4.

We used three plasmids (BR-V108 vector carrying the target sequence, packaging plasmid pMD2.G, and packaging plasmid pSPAX2) for co-transfection. Prior to transfection, 293T cells in the logarithmic growth phase were trypsinised, and their density was adjusted to  $5 \times 10^6$  cells per 15 mL in 10 % FBS medium. Cells were then cultured in a 5 % CO<sub>2</sub> incubator at 37 °C. Transfection commenced when the cell density reached 70 %–80 %. Each DNA solution (BR-V108 plasmid 10 µg, pMD2.G plasmid 7.5 µg, pSPAX2 plasmid 5 µg) was diluted in 500 µL Opti-MEM R1 medium and incubated for 5 min at room temperature. Similarly, Lipofectamine™ 3000 Transfection Reagent was added to another 500 µL Opti-MEM R1 medium and incubated for 5 min at room temperature. The two solutions were mixed thoroughly and allowed to stand at room temperature for 20 min. Subsequently, the mixture was gently added to the 293T cell culture medium and incubated in a cell incubator at 37 °C. After transfection for 72 h, the cell supernatant was collected to obtain a highly purified lentivirus. Cells in logarithmic growth phase were infected under optimal conditions, including a cell MOI (multiple of infection) value of 10, infection with ENL.S (Ecotropic-NIH 3T3 Immortalized Strain) + Polybrene, and a cell count of  $2 \times 10^5$ . Subsequently, the expression of green fluorescent protein was monitored using a fluorescence microscope at 72 h post-infection. Successful infection was determined by fluorescence efficiency exceeding 80 %.

### 2.5. RNA extraction and real-time quantitative PCR (qRT-PCR)

When the cells reached 80 % confluence in a 6-well plate, total RNA was extracted using TRIzol reagent (Sigma, St. Louis, MO, USA), following the manufacturer's instructions. Reverse transcription was performed using the Promega M-MLV Kit (Promega Corporation, Madison, Wisconsin, USA) to generate cDNA. qRT-PCR was performed using a 10 µL reaction volume and the SYBR Green Mastermix Kit (Vazyme, Nanjing, Jiangsu, China). The relative RNA expression was determined using the  $2^{-\Delta\Delta Ct}$  method, with glyceraldehyde 3-phosphate dehydrogenase (GAPDH) serving as the internal control. The primer sequences were as follows (5'–3'): Forward primer of CDC73: 5'-CGCTCCCTTAGAAATAGGTCTTC-3', Reverse primer of CDC73: 5'-CTCTTCATCTCAATTTCGTGGT-3'; Forward primer of GAPDH: 5'-TGACTTCAACAGCGACACCCA-3', Reverse primer of GAPDH: 5'-CACCTGTGTGTAGCCAAA-3'.

### 2.6. Western blot assay

Cells under optimal growth conditions, ranging from  $5 \times 10^5$  to  $1 \times 10^6$ , were harvested and lysed using  $1 \times$  Lysis Buffer (Cell Signal Technology, Danvers, MA). Subsequently, the total proteins were separated via 10 % SDS-PAGE and transferred onto PVDF membranes for Western blot analysis. To minimise non-specific binding, PVDF membranes were treated with a blocking solution (TBS + Tween [TBST] containing 5 % skim milk) at room temperature for 1 h. Primary antibodies were then added, and the membranes were allowed to incubate overnight at 4 °C, followed by addition of secondary antibodies at room temperature for 1 h. Post-incubation, membranes were subjected to three washes with TBST for 10 min each. Protein bands were visualized using the ECL + plus™ Western blotting system kit, followed by X-ray imaging. Details of the antibodies used for western blotting are provided in Supplementary table 1.

### 2.7. Celigo cell counting assay

Eca-109 and TE-1 cells were digested and resuspended to obtain cell suspensions. Each well of a 96-well plate was then seeded with 100 µL of the cell suspension containing 2000 cells, followed by a 5-day incubation period. A Celigo Meter (Nexcelom) was utilized to assess cell density and growth.

### 2.8. CCK-8 assay

After trypsin digestion of ECA-109 cells in the logarithmic growth phase, the cells were resuspended in complete medium to generate a cell suspension. The cells were seeded into a 96-well plate (1000 cells/well) and placed in a cell culture incubator. The following day, 10 µL of CCK-8 reagent was added to each well. After 4 h, the 96-well plate was subjected to oscillation on a shaker for 2–5 min, and the OD was measured at 450 nm using a microplate reader (Tecan Infinite, #M2009PR).

### 2.9. Cell migration assay

To detect cell migration, a Transwell assay was performed. Eca-109 and TE-1 cells, adjusted to a density of  $1 \times 10^5$  cells/mL, were loaded into the upper chamber of a Transwell plate containing serum-free medium. This chamber was subsequently transferred to a lower chamber containing 30 % FBS and incubated for 72 h. After incubation, cells were stained with 400 µL Giemsa, and their migration ability was quantified.

Additionally, a wound-healing assay was conducted. After infection, Eca-109 and TE-1 cells were seeded in 96-well plates at a density of  $5 \times 10^4$  cells/well. The cells were then placed in a 37 °C incubator with 5 % CO<sub>2</sub> and observed under a microscope at 8 h and 48 h. The experiment was repeated three times, and the migration rate of the cells was evaluated based on scratch images.

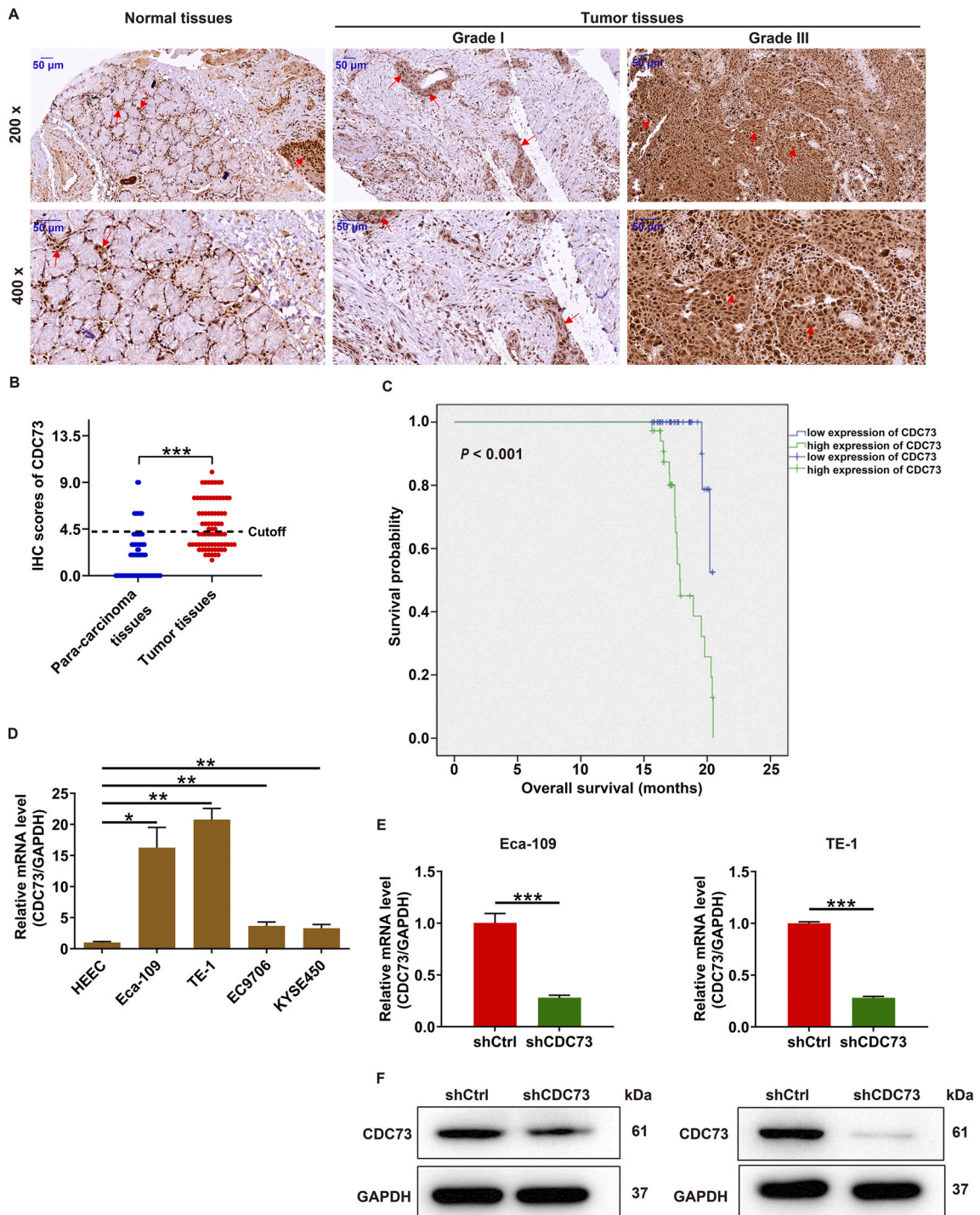


**Fig. 1.** CDC73 expression level is increased in oesophageal cancer. (A) CDC73 protein expression was assessed in oesophageal cancer and para-carcinoma tissues via IHC staining. Arrows indicated CDC73 positive staining. (B) Quantitative plot showing the distribution of CDC73 expression levels across all samples, with the median as the cutoff point. (C) Correlation between CDC73 expression and survival of patients with oesophageal cancer was analysed using Kaplan–Meier survival analysis. (D) Comparative analysis of CDC73 mRNA levels in oesophageal cancer cell lines relative to those in HEEC cells. (E, F) Detection of CDC73 mRNA (E) and protein (F) expression in Eca-109 and TE-1 cells following infection with shCDC73 or shCtrl. \* $P < 0.05$ , \*\* $P < 0.01$ , \*\*\* $P < 0.001$ .

### 2.10. Flow cytometry assay

Eca-109 and TE-1 cells were cultured in 6-well plates, at a volume of 2 mL per well for 5 days. For cell apoptosis analysis, 10  $\mu$ L of Annexin V-APC was added to stain the cells, followed by an incubation period of 10–15 min at room temperature in the dark. The level of apoptosis was quantified using FACSCalibur (BD Biosciences, San Jose, CA, USA). For cell cycle analysis, cells were stained using a staining solution composed of 40  $\times$  PI solution (2 mg/mL), 100  $\times$  RNase solution (10 mg/mL), and 1  $\times$  PBS at a ratio of 25:10:1000. After staining, the cells were analysed using a FACSCalibur (BD Biosciences, San Jose, CA, USA).

### 2.11. Mouse tumour cell xenograft assay

All animal experiments adhered to the European Parliament Directive (2010/63/EU) for the Ethical Treatment of Animals. Mice were randomly divided into groups ( $n = 10$ ), receiving subcutaneous injections of a suspension containing either shCDC73 or shCtrl-infected Eca-109 cells ( $1 \times 10^7$  cells in 100  $\mu$ L PBS). The tumour volume was monitored throughout the feeding period. After 26 days, the mice were euthanised, and the tumours were excised, weighed, and photographed. Tumour samples were frozen in liquid nitrogen ( $-80^\circ\text{C}$ ) for subsequent analysis.

### 2.12. Statistical analysis

Data are expressed as mean  $\pm$  standard deviation (SD) and were analysed using analysis of variance or unpaired t-tests for two-group comparisons. Experiments were performed in triplicate to ensure reproducibility. The Sign test was used to assess differences in CDC73 expression between oesophageal cancer and adjacent tissues. The Mann-Whitney U analysis and Spearman rank correlation analysis were utilized to elucidate the relationship between CDC73 expression levels and patients' pathological features. The association between CDC73 expression and patient survival was evaluated using the Kaplan–Meier survival analysis. Statistical significance was defined as  $P < 0.05$ .

## 3. Results

### 3.1. CDC73 expression level is increased in oesophageal cancer

We conducted an analysis of CDC73 protein expression using an oesophageal cancer tissue microarray. IHC staining revealed a significant increase in CDC73 expression in oesophageal cancer tissues compared to that in adjacent tissues ( $P < 0.001$ , Fig. 1A). The median immunohistochemical staining score for tumour tissues was 4.25. Samples with scores  $\leq 4.25$  were categorised as exhibiting low CDC73 expression, while those with scores  $> 4.25$  were classified as showing high CDC73 expression. Additionally, we generated a quantitative plot illustrating the distribution of CDC73 expression across all samples, using the median as the cutoff point ( $P < 0.001$ , Fig. 1B). The Sign test confirmed a significant increase in CDC73 expression in oesophageal cancer tissues compared to that in adjacent tissues. Among the 78 tumour tissue samples, 50.0 % exhibited high expression, whereas the remaining 50.0 % showed low expression. In contrast, among the 80 para-carcinoma tissue samples, 88.8 % displayed low expression, with only 11.2 % showing high expression ( $P < 0.001$ ; Table 1). Subsequently, we explored the association between CDC73 expression and the clinicopathological characteristics of the patients. Our findings revealed that high CDC73 levels correlated with pathological grade, lymphatic metastasis, and lymph node positivity (Table 2 and Table 3). Moreover, using the Kaplan–Meier survival analysis method, we observed that patients with high CDC73 expression had shorter overall survival than those with low expression levels (Fig. 1C). We assessed CDC73 expression in both normal and oesophageal cancer cell lines. The results showed significant upregulation of CDC73 in oesophageal cancer cell lines compared to that in normal cells (Fig. 1D). Based on these results, we concluded that CDC73 could function as a tumour-promoting factor in the development of oesophageal cancer.

### 3.2. Knockdown of CDC73 inhibits the growth of oesophageal cancer cells in vitro

To explore the functional roles of CDC73 in oesophageal cancer cell growth, we infected Eca-109 and TE-1 cells with short hairpin structures expressing CDC73 (shCDC73) or the vector shCtrl. Successful infection was validated using qRT-PCR and western blotting (Fig. 1E and F and S1A). Subsequently, we evaluated cell activity using the Celigo cell counting assay and observed a significant inhibition of cell activity upon CDC73 depletion in both Eca-109 and TE-1 cells (Fig. 2A). Next, we investigated the cell migration capacity using a wound-healing assay, which revealed that CDC73 knockdown attenuated cell migration (Fig. 2B). Consistently, Transwell assays indicated a notable reduction in the number of migrated Eca-109 and TE-1 cells in the basolateral chamber following

**Table 1**  
Expression patterns in esophagus cancer tissues and para-carcinoma tissues revealed in immunohistochemistry analysis.

CDC73 expression	Tumor tissue		Para-carcinoma tissue		P value $P < 0.001$
	Cases	Percentage	Cases	Percentage	
Low	39	50.0 %	71	88.8 %	
High	39	50.0 %	9	11.2 %	

**Table 2**  
Relationship between CDC73 expression and tumor characteristics in patients with esophagus cancer.

Features	No. of patients	CDC73 expression		P value
		low	high	
All patients	78	39	39	
Age (years)	78	39	39	0.121
Gender				0.392
Male	63	33	30	
Female	15	6	9	
Tumor size	70	35	35	0.109
Tumor infiltrate				0.586
T0	1	1	0	
T1	2	0	2	
T2	10	6	4	
T3	31	15	16	
T4	12	5	7	
lymphatic metastasis (N)				0.009
N0	19	14	5	
N1	16	6	10	
N2	12	5	7	
N3	9	2	7	
Stage				0.153
I	2	1	1	
II	18	12	6	
III	33	12	21	
IV	3	2	1	
Lymphoid positive number	77	39	38	0.031
Grade				0.029
I	7	6	1	
II	38	21	17	
III	24	9	15	

**Table 3**  
Relationship between CDC73 expression with pathological grade, lymphoid positive number and lymphatic metastasis in patients with esophagus cancer.

		CDC73
Grade	Spearman correlation	0.266
	Signification (double-tailed)	0.027
	N	69
Lymphoid positive number	Spearman correlation	0.248
	Signification (double-tailed)	0.030
	N	77
lymphatic metastasis (N)	Spearman correlation	0.352
	Signification (double-tailed)	0.008
	N	56

CDC73 depletion (Fig. 2C). We also explored the effects of CDC73 knockdown on apoptosis and cell cycle progression using flow cytometry. The data illustrated that silencing of CDC73 significantly increased the percentage of apoptotic cells in both Eca-109 and TE-1 cells (Fig. 2D). Furthermore, cell cycle analysis revealed that CDC73 depletion led to G2 phase cell cycle arrest (Fig. 2E). In summary, these findings collectively demonstrated that the depletion of CDC73 resulted in decreased cell activity, impaired migration, enhanced apoptosis, and G2 phase cell cycle arrest.

### 3.3. Knockdown of CDC73 inhibits the outgrowth of oesophageal cancer cells *in vivo*

To delve deeper into the impact of CDC73 on oesophageal cancer cell growth *in vivo*, we conducted a subcutaneous injection study employing Eca-109 cells with stable CDC73 downregulation or the shCtrl vector in nude mice. Our results revealed that CDC73 downregulation significantly impeded the growth rate of tumours formed by Eca-109 cells in nude mice (Fig. 3A-C). Furthermore, a conspicuous reduction in CDC73 levels was observed in tumour tissues obtained from mice injected with Eca-109 cells exhibiting CDC73 downregulation (Fig. 3D and S1B). To ascertain CDC73 expression in tumours, we performed IHC, which revealed a significant decrease in the staining intensity of CDC73 in tumours derived from CDC73-deficient cells (Fig. 3E). These collective findings strongly indicated that silencing CDC73 disrupted tumour outgrowth in oesophageal cancer *in vivo*.

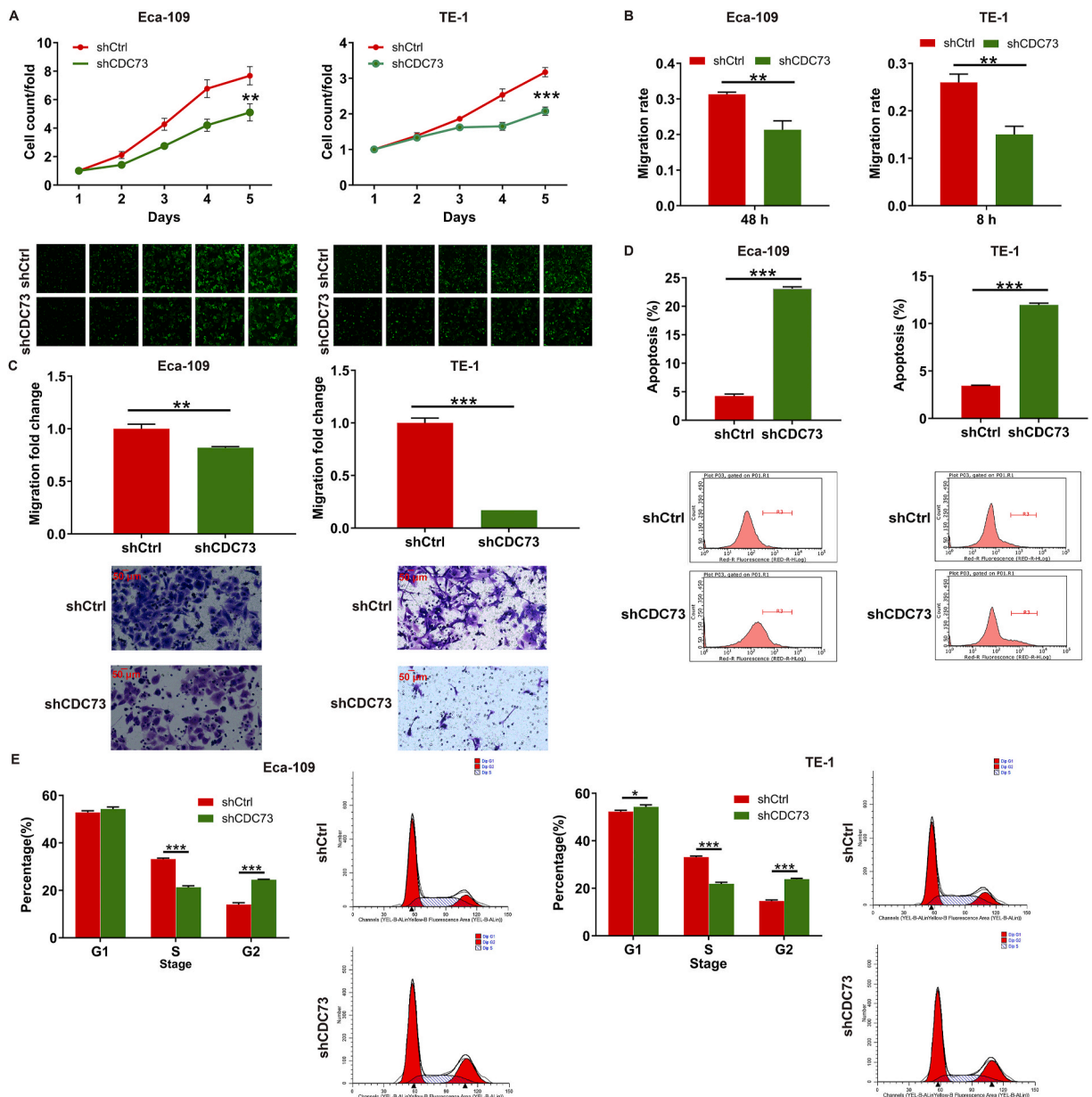


**Fig. 2.** Knockdown of CDC73 inhibits the growth of oesophageal cancer cells *in vitro*. (A) Assessment of cell proliferation in Eca-109 and TE-1 cells following infection with shCDC73 or shCtrl. (B, C) Evaluation of cell migration using wound-healing assay (B) and Transwell analysis (C) in Eca-109 and TE-1 cells after CDC73 knockdown. (D, E) The effects of CDC73 depletion on apoptosis (D) and cell cycle progression (E) were visualized using flow cytometry in Eca-109 and TE-1 cells. \* $P < 0.05$ , \*\* $P < 0.01$ , \*\*\* $P < 0.001$ .

### 3.4. CDC73 regulates oesophageal cancer through RRP15

In this segment of our investigation, we conducted a preliminary exploration of the mechanism by which CDC73 influences oesophageal cancer. Utilising data from the Coexpedia website ([https://www.coexpedia.org/hs\\_single.php?gene=CDC73](https://www.coexpedia.org/hs_single.php?gene=CDC73)), we identified the top five genes co-expressed with CDC73—NSL1, MARCH7, RPAP3, UCHL5, and RRP15—ranked by the sum of their edge’ LLS scores (Fig. 4A). Subsequently, we knocked down these genes and assessed their impact on Eca-109 cell proliferation using a CCK-8 assay. Remarkably, the results revealed that the knockdown of all genes significantly inhibited cell proliferation compared to that in the shCtrl group, with RRP15 demonstrating the most pronounced inhibitory effect among the tested genes, implying that RRP15 could be a target of CDC73 (Fig. 4B). To delve deeper into the potential association between CDC73 and RRP15, we analysed 162 ESCA samples using the ENCORI Pan-Cancer Analysis Platform (<https://rna.syu.edu.cn/encori/panCancer.php>). The analysis revealed a positive correlation between CDC73 and RRP15 expression (Fig. 4C). Additionally, we observed elevated RRP15 levels in oesophageal

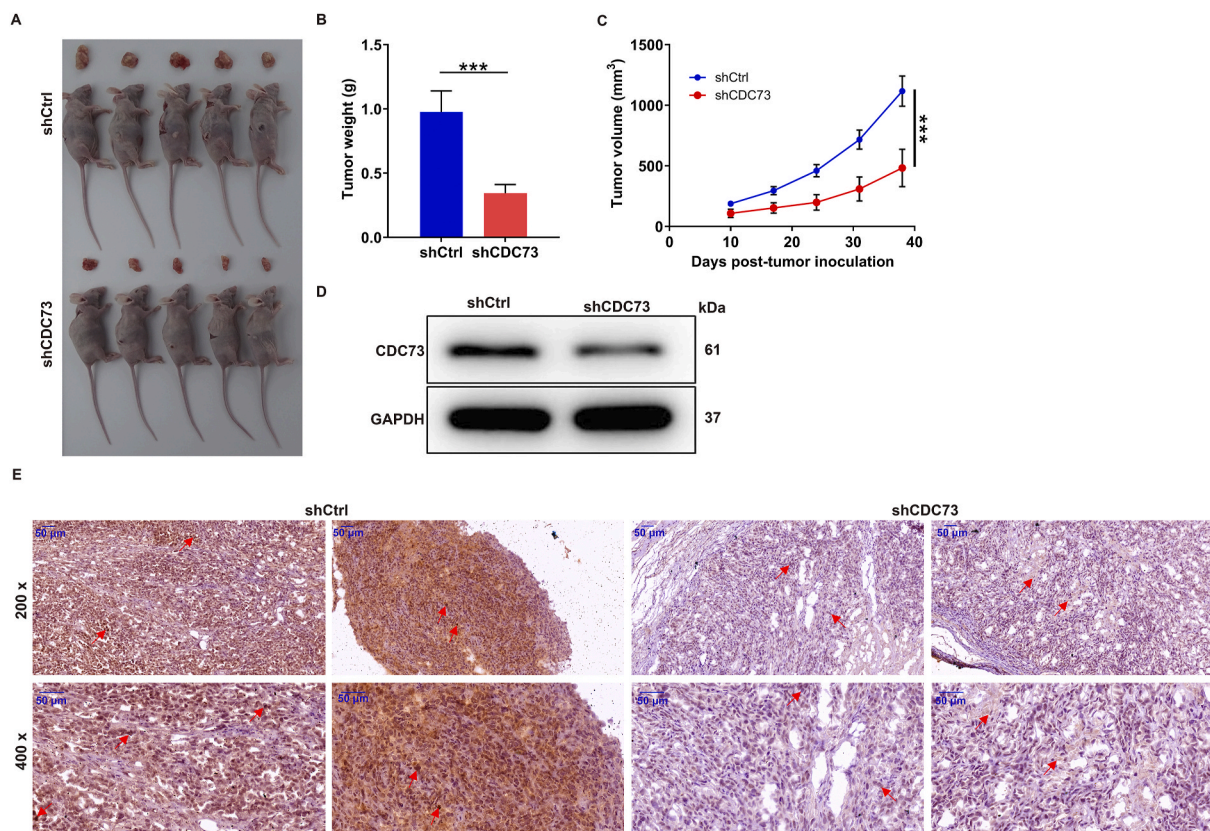


**Fig. 3.** Knockdown of CDC73 inhibits the outgrowth of oesophageal cancer cells *in vivo*. (A) Representative images of tumours derived from shCtrl/shCDC73-infected Eca-109 cells. (B, C) Measurement of tumour weight (B) and volume (C) at the indicated time points. (D, E) Detection of CDC73 protein levels in tumour tissues from mice injected with shCtrl/shCDC73-infected Eca-109 cells using Western blot (D) and IHC staining (E). Arrows indicated CDC73 positive staining. \*\*\* $P < 0.001$ .

cancer cell lines compared to those in HEEC (Fig. 4D). Subsequently, we assessed the mRNA levels of RRP15 in both overexpressed and silenced CDC73, Eca-109, and TE-1 cells. As anticipated, the upregulation of CDC73 led to an increase in RRP15 mRNA expression, whereas the depletion of CDC73 resulted in its decrease (Fig. 4E). To further elucidate the involvement of CDC73 and RRP15 in the development of oesophageal cancer, we conducted a series of rescue experiments. Our findings indicated that heightened CDC73 expression accelerated the proliferation and migration of Eca-109 and TE-1 cells. Notably, knockdown of RRP15 hindered cell growth and movement and even counteracted the promoting effects of CDC73 overexpression (Fig. 4F-H). Collectively, these results suggest that CDC73 upregulated RRP15 to induce malignant phenotypes in oesophageal cancer.

#### 4. Discussion

Oesophageal cancer is one of the top ten lethal cancers globally because of its highly aggressive nature and poor survival rate [14]. Surgery, the primary treatment modality, is feasible in approximately 20 % of patients with oesophageal cancer [15]. Complementary approaches, such as radiotherapy and chemotherapy, have also been employed. However, conventional chemotherapeutic agents have exhibited limited efficacy in clinical trials and are often accompanied by severe side effects [16]. The pursuit of targeted therapies for oesophageal cancer has generated considerable interest. Despite their potential to enhance treatment outcomes, drug resistance remains a challenge [3,4]. Hence, there is a pressing need to explore novel therapeutic strategies with improved efficacy and minimal adverse effects to combat oesophageal cancer.

In the current study, we evaluated the CDC73 mRNA levels in four human oesophageal cancer cell lines. Although all four cell lines exhibited significant upregulation of CDC73 compared to that in HEEC, the disparity in expression levels among EC9706, KYSE450, Eca-109, and TE-1 warrants further investigation. Several factors may have contributed to this discrepancy. Firstly, it is essential to consider the inherent heterogeneity of cancer cell populations, even within the same cancer type. Each cell line may represent a distinct subtype of oesophageal cancer with unique genetic and molecular characteristics. EC9706, KYSE450, and TE-1 cells originate from squamous cell carcinomas, whereas Eca-109 cells originate from adenocarcinomas. Each cell line possesses unique characteristics that reflect its subtype and influence its proliferation rate, invasive potential, and molecular profile. Although EC9706, KYSE450, and TE-1 cells originate from the same subtype, cellular and tumour microenvironments can profoundly influence their gene expression



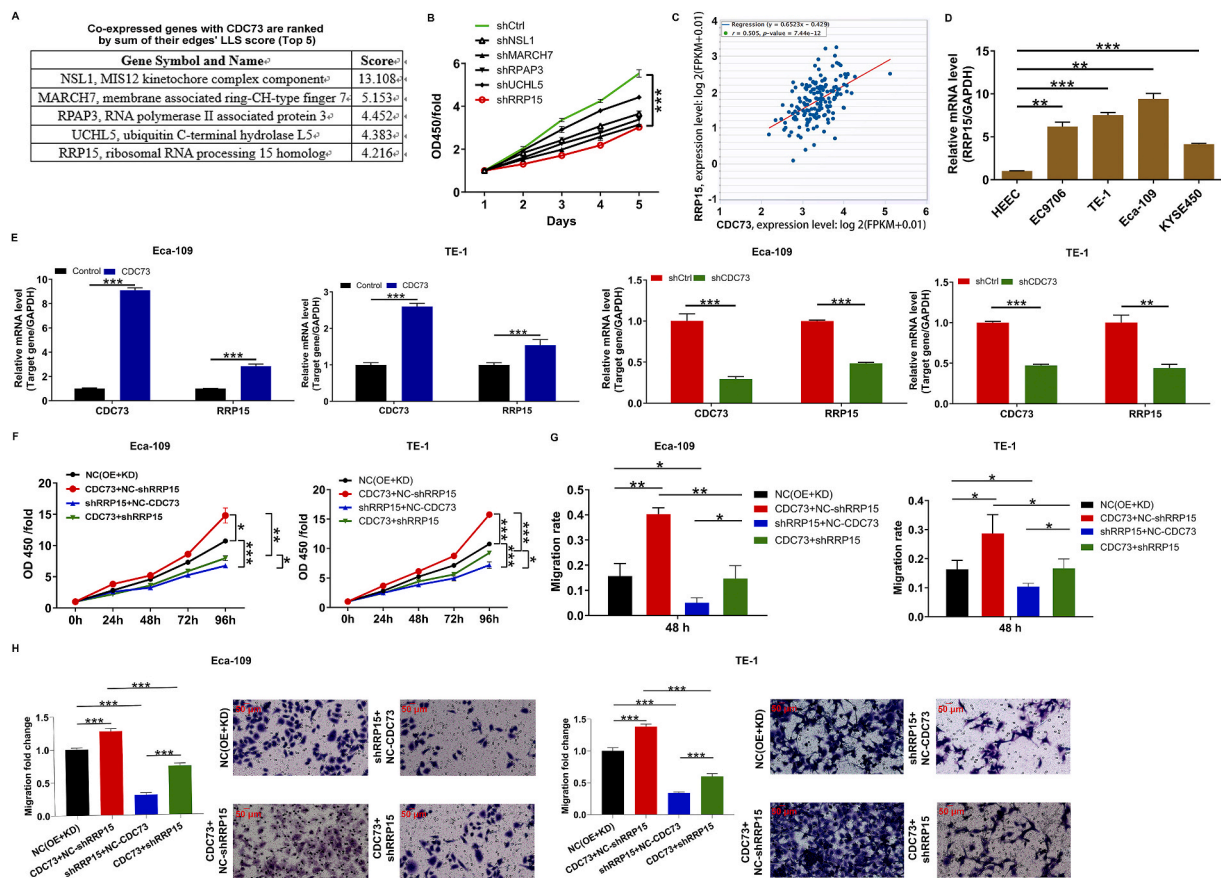


**Fig. 4.** CDC73 regulates oesophageal cancer through RRP15. (A) The top 5 genes co-expressed with CDC73 were ranked based on the sum of the LLS scores. (B) Impact of NSL1, MARCH7, RPAP3, UCHL5, and RRP15 knockdown on Eca-109 cell proliferation assessed via CCK-8 assay. (C) Correlation analysis between CDC73 and RRP15 in 162 ESCA samples from the ENCORI Pan-Cancer Analysis Platform. (D) Comparative analysis of RRP15 mRNA levels in oesophageal cancer cell lines relative to those in HEEC cells. (E) Evaluation of RRP15 mRNA levels in both CDC73-overexpressed and silenced Eca-109 and TE-1 cells using qRT-PCR. (F) Assessment of cell proliferation in Eca-109 and TE-1 cells from four groups: NC (OE + KD), CDC73 + NC-shRRP15, shRRP15 + NC-CDC73, CDC73 + shRRP15. (G, H) Evaluation of cell migration abilities by conducting wound-healing assay (G) and Transwell analysis (H) with Eca-109 and TE-1 cells from the four aforementioned groups. \* $P < 0.05$ , \*\* $P < 0.01$ , \*\*\* $P < 0.001$ . NC (OE + KD): Control; CDC73 + NC-shRRP15: CDC73 overexpression; shRRP15 + NC-CDC73: RRP15 downregulation; CDC73 + shRRP15: CDC73 overexpression and RRP15 downregulation.

patterns [17]. Hypoxia, nutrient availability, and stromal cell interactions selectively enhance or suppress CDC73 expression in certain cell lines [18,19]. Additionally, epigenetic modifications, including DNA methylation and histone acetylation, modulate CDC73 expression in a cell type-specific manner [20,21]. These differences underscore the importance of considering tumour heterogeneity in experimental research and therapeutic development of oesophageal cancer.

Moreover, we noted a significant upregulation of CDC73 in oesophageal cancer tissues, which correlated with patient prognosis. Initially identified as a tumour suppressor gene, CDC73 has been implicated in various cancer-related pathways. For instance, CDC37 downregulates the expression of cyclin D1 [22,23] and c-myc proto-oncogene [24]. In breast cancer, CDC73 expression negatively correlates with disease progression [25]. Moreover, HSF2BP overexpression has been linked to reduced endoplasmic reticulum (ER) stress by elevating cytoplasmic CDC73 levels and inhibiting the JNK signalling pathway, suggesting a potential therapeutic avenue for hepatocyte ER stress-related conditions [26]. Additionally, Rather et al. reported CDC73 downregulation in oral squamous cell carcinoma, suggesting therapeutic implications for disease management [27]. However, there have been instances in which CDC73 exhibits oncogenic functions. For example, CDC73 is significantly overexpressed in hepatocellular carcinoma (HCC), and its inhibition leads to suppressed cell proliferation, G1 phase cell cycle arrest, and increased cell apoptosis [28]. Furthermore, USP37 acts as a deubiquitinating enzyme for CDC73, promoting its stability in HPT-JT syndrome [29]. Notably, the conditional deletion of CDC73 in mature osteoblasts and osteocytes results in altered bone density and remodelling, emphasising its role in bone homeostasis and gene expression regulation [30]. In our study, we observed that CDC73 knockdown inhibited the viability and migration of oesophageal cancer cells and restrained the growth of xenograft tumours. Based on these findings, we proposed that CDC73 functions as a cancer-promoting factor in oesophageal cancer. Notably, the knockdown of CDC73 had a lesser effect on Eca-109 than on TE-1 cells, as assessed at different time points (48 h for Eca-109 and 8 h for TE-1). Several factors account for this observation. Firstly, it is important

to note that different cell lines may exhibit variations in migratory behaviour because of inherent genetic differences or phenotypic characteristics. Eca-109 and TE-1 cells originate from distinct subtypes of oesophageal cancer, potentially displaying differences in molecular characteristics, such as gene and protein expression, as well as migratory capabilities. Moreover, the cell growth rates vary among different cell lines. Eca-109 cells may reach sufficient confluence and exhibit noticeable migratory behaviour after 48 h, whereas TE-1 cells may require a shorter duration (8 h) owing to their faster growth kinetics or higher baseline migratory activity. These variations may lead to divergent cellular responses and behaviours. Therefore, it is plausible that the observed differences in the effects of CDC73 knockdown on the migration assays could be attributed to inherent variances between the two cell lines.

In addition to investigating the effect of CDC73 on oesophageal cancer, we explored the underlying mechanism by examining its co-expressed genes and validating their expression in oesophageal cancer samples. Our findings revealed a positive correlation between CDC73 and RRP15, indicating that RRP15 is a potential target of CDC73. RRP15 is a protein localised in the cell nucleus that plays a crucial role in the processing of ribosomal RNA, including mRNA and rRNA, as well as in the activity of the 20S proteasome in cells [31]. Previous studies have highlighted the role of RRP15 in various malignancies. For instance, RRP15 has been found to be upregulated in HCC cell lines and tumours, and its increased expression in HCC tumours was associated with an unfavourable prognosis [32]. RRP15 has also been implicated in the regulation of cell cycle, proliferation, and apoptosis of T cells [33]. Our results demonstrated that the knockdown of RRP15 suppressed cell proliferation and migration and reversed the promoting effects of CDC73 overexpression in oesophageal cancer.

In summary, this study offers new insights into the functional role of CDC73 in oesophageal cancer development. Our findings highlighted CDC73-induced promotion of malignant progression in oesophageal cancer through the upregulation of RRP15, suggesting CDC73 as a potential therapeutic target for oesophageal cancer treatment. The identification of CDC73 as a potential therapeutic target unveils new opportunities for interventions in oesophageal cancer treatment. Understanding role of CDC73 in tumorigenesis and its interactions within oesophageal cancer progression pathways has paved the way for targeted therapies to disrupt or modulate its function. We aimed to bridge the gap between basic research and clinical practice, thereby enhancing the relevance and impact of this study. Further exploration and validation of CDC73 as a therapeutic target in clinical settings show promise for improving treatment outcomes and patient prognosis in the management of oesophageal cancer.

Our research encompassed various histological subtypes of oesophageal cancer, ensuring broad applicability. We conducted cell experiments using Eca-109 and TE-1 cells, which represent oesophageal squamous cell carcinoma and adenocarcinoma, respectively. Moreover, the oesophageal cancer tissue microarray utilized in our study included diverse subtypes, such as squamous cell carcinoma, adenocarcinoma, and small cell carcinoma. However, it is important to acknowledge the limitations of this study. Specifically, our exploration of the regulatory mechanisms underlying the CDC73-mediated modulation of RRP15 remains preliminary and warrants further investigation.

### **Ethical approval**

The study involving human was approved by Ethical Committee of Shanghai Outdo Biotech Company (No. SHYJS-CP-1407005). The animal experiments was approved by Laboratory Animal Ethics Committee of Ningbo University (No. NBU20220097).

### **Informed consent from participants**

Signed informed consents were provided by all patients.

### **Data availability statement for Share upon Reasonable Request data Sharing Policy clinical trial registration**

The data set supporting the results of this article are included within the article.

### **Funding**

This work was financially supported by Zhejiang Traditional Chinese Medicine Administration (No. 2024ZL944)

### **CRedit authorship contribution statement**

**Jie Song:** Writing – review & editing, Writing – original draft, Resources, Methodology, Funding acquisition. **Wenyong Guo:** Writing – review & editing, Writing – original draft, Resources, Methodology. **Hua Xu:** Supervision, Resources, Project administration. **Tao Gao:** Formal analysis, Conceptualization.

### **Declaration of competing interest**

The authors declare that they have no known competing financial interests or personal relationships that could have appeared to influence the work reported in this paper.

## Acknowledgement

None.

## Appendix A. Supplementary data

Supplementary data to this article can be found online at <https://doi.org/10.1016/j.heliyon.2024.e29904>.

## References

- [1] C.C. Abnet, M. Arnold, W.-Q. Wei, Epidemiology of esophageal squamous cell carcinoma, *Gastroenterology* 154 (2) (2018) 360–373, <https://doi.org/10.1053/j.gastro.2017.08.023>.
- [2] F.-L. Huang, S.-J. Yu, Esophageal cancer: Risk factors, genetic association, and treatment, *Asian J. Surg.* 41 (3) (2018) 210–215, <https://doi.org/10.1016/j.asjsur.2016.10.005>.
- [3] A.F. Hassanabad, R. Chehade, D. Breadner, et al., Esophageal carcinoma: towards targeted therapies, *Cell. Oncol.* 43 (10) (2019).
- [4] YM Yang, P Hong, WW Xu, et al., Advances in targeted therapy for esophageal cancer, *Signal Transduct Target Ther* 5 (1) (2020 Oct 7) 229, <https://doi.org/10.1038/s41392-020-00323-3>.
- [5] W. Sun, X.L. Kuang, Y.P. Liu, et al., Crystal structure of the N-terminal domain of human CDC73 and its implications for the hyperparathyroidism-jaw tumor (HPT-JT) syndrome, *Sci. Rep.* 7 (1) (2017) 15638, <https://doi.org/10.1038/s41598-017-15715-9>.
- [6] P.J. Newey, M.R. Bowl, R.V. Thakker, Parafibromin—functional insights, *J. Intern. Med.* 266 (1) (2009) 84–98, <https://doi.org/10.1111/j.1365-2796.2009.02107.x>.
- [7] J.D. Carpten, C.M. Robbins, A. Villablanca, et al., HRPT2, encoding parafibromin, is mutated in hyperparathyroidism-jaw tumor syndrome, *Nat. Genet.* 32 (4) (2002) 676–680, <https://doi.org/10.1038/ng1048>.
- [8] P.J. Newey, M.R. Bowl, T. Cranston, et al., Cell division cycle protein 73 homolog (CDC73) mutations in the hyperparathyroidism-jaw tumor syndrome (HPT-JT) and parathyroid tumors, *Hum. Mutat.* 31 (3) (2010) 295–307, <https://doi.org/10.1002/humu.21188>.
- [9] A.J. Gill, Understanding the genetic basis of parathyroid carcinoma, *Endocr. Pathol.* 25 (1) (2014) 30–34, <https://doi.org/10.1007/s12022-013-9294-3>.
- [10] J. Zhao, A. Yart, S. Frigerio, et al., Sporadic human renal tumors display frequent allelic imbalances and novel mutations of the HRPT2 gene, *Oncogene* 26 (23) (2007) 3440–3449, <https://doi.org/10.1038/sj.onc.1210131>.
- [11] F. Cetani, C. Banti, E. Pardi, et al., CDC73 mutational status and loss of parafibromin in the outcome of parathyroid cancer, *Endocr Connect* 2 (4) (2013) 186–195, <https://doi.org/10.1530/EC-13-0046>.
- [12] Y. E, H. Xue, C.Y. Zhang, et al., The clinicopathological and prognostic significances of CDC73 expression in breast cancer: a pathological and bioinformatics analysis, *Histol. Histopathol.* (2022) 18534, <https://doi.org/10.14670/HH-18-534>.
- [13] S.M. Hyde, T.A. Rich, S.G. Waguespack, et al., CDC73-Related disorders, in: M.P. Adam, D.B. Everman, G.M. Mirzaa, R.A. Pagon, S.E. Wallace, L.J.H. Bean, K. W. Gripp, A. Amemiya (Eds.), *GeneReviews(R)*, Seattle (WA), 1993.
- [14] F Bray, J Ferlay, I Soerjomataram, et al., Global cancer statistics 2018: GLOBOCAN estimates of incidence and mortality worldwide for 36 cancers in 185 countries, *CA Cancer J Clin* 68 (6) (2018 Nov) 394–424, <https://doi.org/10.3322/caac.21492>.
- [15] G.D. Eslick, Epidemiology of esophageal cancer, *Gastroenterol. Clin. N. Am.* 38 (1) (2009) 17–25, <https://doi.org/10.1016/j.gtc.2009.01.008>.
- [16] A. Joe, D.K. Agrawal, S.K. Mittal, Targeted chemotherapy for esophageal cancer, *Front. Oncol.* 7 (2017) 63.
- [17] D.F. Quail, J.A. Joyce, Microenvironmental regulation of tumor progression and metastasis, *Nat Med* 19 (11) (2013) 1423–1437, <https://doi.org/10.1038/nm.3394>.
- [18] N.N. Pavlova, C.B. Thompson, The emerging hallmarks of cancer metabolism, *Cell Metab.* 23 (1) (2016) 27–47, <https://doi.org/10.1016/j.cmet.2015.12.006>.
- [19] G. Yang, R. Shi, Q. Zhang, Hypoxia and oxygen-sensing signaling in gene regulation and cancer progression, *Int. J. Mol. Sci.* 21 (21) (2020), <https://doi.org/10.3390/ijms21218162>.
- [20] A.P. Feinberg, B. Vogelstein, Hypomethylation distinguishes genes of some human cancers from their normal counterparts, *Nature* 301 (5895) (1983) 89–92, <https://doi.org/10.1038/301089a0>.
- [21] S.B. Baylin, P.A. Jones, A decade of exploring the cancer epigenome - biological and translational implications, *Nat. Rev. Cancer* 11 (10) (2011) 726–734, <https://doi.org/10.1038/nrc3130>.
- [22] G.E. Woodard, L. Lin, J.H. Zhang, et al., Parafibromin, product of the hyperparathyroidism-jaw tumor syndrome gene HRPT2, regulates cyclin D1/PRAD1 expression, *Oncogene* 24 (7) (2005) 1272–1276, <https://doi.org/10.1038/sj.onc.1208274>.
- [23] Y.J. Yang, J.W. Han, H.D. Youn, et al., The tumor suppressor, parafibromin, mediates histone H3 K9 methylation for cyclin D1 repression, *Nucleic Acids Res.* 38 (2) (2010) 382–390, <https://doi.org/10.1093/nar/gkp991>.
- [24] L. Lin, J.H. Zhang, L.M. Panicker, et al., The parafibromin tumor suppressor protein inhibits cell proliferation by repression of the c-myc proto-oncogene, *Proc Natl Acad Sci U S A* 105 (45) (2008) 17420–17425, <https://doi.org/10.1073/pnas.0710725105>.
- [25] G. Xiang, S. Wang, L. Chen, et al., UBR5 targets tumor suppressor CDC73 proteolytically to promote aggressive breast cancer, *Cell Death Dis.* 13 (5) (2022) 451, <https://doi.org/10.1038/s41419-022-04914-6>.
- [26] J. Zhang, T. Wang, J. Bi, et al., Overexpression of HSF2 binding protein suppresses endoplasmic reticulum stress via regulating subcellular localization of CDC73 in hepatocytes, *Cell Biosci.* 13 (1) (2023) 64, <https://doi.org/10.1186/s13578-023-01010-w>.
- [27] M.I. Rather, M.N. Nagashri, S.S. Swamy, et al., Oncogenic microRNA-155 down-regulates tumor suppressor CDC73 and promotes oral squamous cell carcinoma cell proliferation: implications for cancer therapeutics, *J. Biol. Chem.* 288 (1) (2013) 608–618, <https://doi.org/10.1074/jbc.M112.425736>.
- [28] Z. Wang, W. Wei, C.K. Sun, et al., Suppressing the CDC37 cochaperone in hepatocellular carcinoma cells inhibits cell cycle progression and cell growth, *Liver Int.* 35 (4) (2015) 1403–1415, <https://doi.org/10.1111/liv.12651>.
- [29] S.Y. Kim, J.Y. Lee, Y.J. Cho, et al., USP37 deubiquitinates CDC73 in HPT-JT syndrome, *Int. J. Mol. Sci.* 23 (12) (2022), <https://doi.org/10.3390/ijms23126364>.
- [30] C.J. Droscha, C.R. Diegel, N.J. Ethen, et al., Osteoblast-specific deletion of Hrpt2/Cdc73 results in high bone mass and increased bone turnover, *Bone* 98 (2017) 68–78, <https://doi.org/10.1016/j.bone.2016.12.006>.
- [31] H. Tschochner, E. Hurt, Pre-ribosomes on the road from the nucleolus to the cytoplasm, *Trends Cell Biol.* 13 (5) (2003) 255–263, [https://doi.org/10.1016/s0962-8924\(03\)00054-0](https://doi.org/10.1016/s0962-8924(03)00054-0).
- [32] D. Zhao, L. Qian, D. Zhuang, et al., Inhibition of ribosomal RNA processing 15 Homolog (RRP15), which is overexpressed in hepatocellular carcinoma, suppresses tumour growth via induction of senescence and apoptosis, *Cancer Lett.* 519 (2021) 315–327, <https://doi.org/10.1016/j.canlet.2021.07.046>.
- [33] T. Wu, M.X. Ren, G.P. Chen, et al., Rrp15 affects cell cycle, proliferation, and apoptosis in NIH3T3 cells, *FEBS Open Bio* 6 (11) (2016) 1085–1092, <https://doi.org/10.1002/2211-5463.12128>.